Exploding wire energy absorption dynamics at slow current rates.

G. Rodríguez Prieto [*a], L. Bilbao[b], and M. Milanese[c]

[a] Universidad de Castilla-la Mancha, I.N.E.I., 13071, Ciudad Real, Spain

[b] Instituto de Física del Plasma, UBA-CONICET, 1428, Buenos Aires, Argentina

[c] CONICET, Universidad Nacional del Centro de la Provincia de Buenos Aires, Instituto de Física Arroyo Seco - Facultad de Ciencias Exactas, 7000, Tandil, Argentina

Pages 25

Tables 1

Figures 10

[*]E-mail: gonzalo.rprieto@uclm.es

Phone: 0034 926 295 300 Ext. 96628

Exploding wire energy absorption dynamics at slow current rates.

Abstract

Absorption of electrical energy provided to a metal wire in an exploding wire system is thought to be terminated or greatly diminished when the plasma is formed, after the Joule heating of the metallic wire by the electrical current. Accordingly, it is common to account for the electrical energy delivered to the wire that the integration of current and voltage signals is halted when the voltage peak changes its slope. Usually, this moment is synchronized with the plasma appearance in optical sensors. In this work experimental evidence of a two steps electrical energy absorption in an exploding wire surrounded by atmospheric air is presented. Meanwhile in the first step of the energy absorption the plasma is not formed, during the second step the plasma is already expanding. Delay between the two steps can reach ≈2.2 μs for copper wires of 50 μm diameter charged with an initial voltage of 10 kV. The relation of the current density with the initial kinetic energy of the plasma and the electrical current is developed as a possible explanation of the observed phenomena.

Keywords Exploding wires; Energy absorption dynamics.

1 Introduction

When a high, fast current flows through a metallic wire, the wire heats rapidly by joule effect, changing its state from solid to liquid and then gas, to finally become plasma. If the current is released in a controlled manner, the exploding wire system is used as an experimental platform for plasma generation and many associated research fields (Ram and Sadot, 2012; Stephens et al., 2012; Sheftman and Krasik, 2010; Sarathi et al., 2009). Despite of the fact that the experiment of a current passing through a conductor has been studied from the end of the eighteenth century (Nairne, 1780), it is after the middle of twentieth century that the exploding wire phenomenon has beeen studied with more powerful measurement systems, as the review of Bennett (Bennett et al., 1969) demonstrates. Along its history and until present times, scientific use of exploding wires covers a broad range of topics. Some examples are the experimental observation of metallic properties near boiling points (Chandler et al., 2002), the generation of high pressure shock waves on a dense medium, specifically in water (Sasaki et al., 2006; Efimov et al., 2008; Krasik et al., 2008), and the use of exploding wires as substitutes of explosives in the generation and study of blast waves (Liverts et al., 2015; Ram and Sadot, 2012). Also, carefully choosing the exploding wire parameters implies that some states of matter can be experimentally observed, such as their liquid state (Kuskova et al., 1997), and therefore material properties of metals could be compared with theoretical predictions (DeSilva and Katsouros, 1998; Sheftman and Krasik, 2010; Beilis et al., 2009).

To reach conclusions on the resulting plasma of an exploding wire, a fundamental parameter is the energy density deposition from the electrical circuit to the wire-plasma system. This energy deposition is very sensitive to the electrical current rate, as it has been demonstrated in previous experiments (Sarkisov et al., 2004). To be able to perform measurements on the energy deposition, the most direct way is the use of experimentally obtained voltage and current signals on the wire. Combination of these measurements with radial expansion dynamics allow for the exploration of the plasma parameters, so the comparison of experimental and simulated electrical waveforms are used frequently as benchmarks of codes and their conductivity models, therefore many examples can be found in the literature (Stephens and Neuber, 2012; Beilis et al., 2008; Gurovich et al., 2004).

In this work we present results for exploding wires of different metals with a current rate below 12 A/ns in atmospheric air. This value indicates a relative slow current rate in comparison with other works already published, were their current rates could be so large as 500 A/ns Sheftman and Krasik (2010). Experiments and simulations that show a complex interplay between

the energy absorption and the current density are also presented in this work. They show an excellent agreement between the theoretical and experimental waveforms of the voltage and current values.

This paper is structured as follows. After this introduction, the experimental setup and numerical methods are explained in the two following sections. Experimental and simulation results are presented later, and a last section of conclusions ends this work.

2 Experimental Setup and Methods

Experiments were performed with the ALEX system (Alambre Explosivo, in Spanish), a typical exploding wire setup, formed by a two capacitors bank (1.13 μF, 40 nH each) connected in parallel with a high voltage source. A wire is attached in series between the spark-gap and the ground, having an inductance of 140 nH. Wires are of fixed length (3 cm) and surrounded by atmospheric air, but with different metals and diameters, see table 1. Heat content data presented in the table had been obtained from Pankratz and Mrazek (1983). The initial voltage of the capacitor bank varied from 10 to 25 kV (in steps of 5 kV).

In figure 1 the equivalent electrical circuit of the setup is shown, where the total inductance of the capacitors has been enclosed as a single component. Measurement of the time evolution of the energy delivered by the circuit to the wire has been obtained by recording the signals from a resistive voltage divider and a Rogowsky coil, placed in the locations indicated in the figure 2. Also the plasma radial expansion is simultaneously measured as a function of time during the wire explosion time. Electrical probes has been designed and calibrated in our laboratory. The signals are transmitted through coaxial cables to the oscilloscopes, shielded against electromagnetic noise in a Faraday cage. Numerical integration of the Rogowsky signals gives the current that flows through the wire. To observe the plasma expansion, a streak image system was focused on the wire for recording the self-emitted plasma light. A fast photodiode, directed towards the wire, was used for the synchronization of the electrical signals with the optical images of the streak system, see figure 2 for the scheme of the experimental setup.

Recorded signals from the voltage divider corresponds to the sum of the exploding wire voltage drop plus that of the electrodes and connections in series with the wire. In order to remove from the signals the unwanted voltage drop, i.e, that of electrodes and connectors, a common practice is to use an ad–hoc approximation of the behaviour of this part of the circuit by just a

constant inductance. Thus the voltage across the wire is obtained as the difference between measured voltage and that of the modeled inductance.

We have instead used a different approach. As a matter of fact, the late oscillatory part of the signal (late in time, after formation and evolution of the plasma) is well fitted by two constant circuit elements, one inductive and other resistive. Notice that the inductance and resistivity of the fitting are taken at latter times in the wire explosion, after its disappearance and they are different from the initial values. Therefore, the voltage drop on the wire is obtained by subtracting, from the measured signal, the previous fit. As an example, in figure 3 we show the result of this procedure for a tungsten wire with a diameter of 100 μm and initial voltage of 15 kV. Further, the numerical simulation which is described below, supports this approach.

From voltage and current across the exploding wire, we obtain the electrical power and the energy delivered to the wire. Furthermore, assuming cylindrical symmetry, the combination of the electrical current data with the radial expansion of the plasma, leads to a lower limit for the wire resistivity as a function of time obtained as (Rodríguez Prieto et al., 2016):

$$\mu \leq \mu_{min} = \frac{\Delta V \ S_w}{I \ l_w}, \tag{1}$$

where ΔV is the measured voltage along the wire, S_w the wire section, I the wire current and l_w the wire length.

Of the recorded streak images, plasma radial dynamics is obtained by a simple method. Plasma radial border is defined as the position where the intensity is 5% of the maximum recorded value on the streak image for each experiment. This is searched sequentially for each time instant and calibrated in space and time to obtain the final radial expansion, that is then fitted by the function (Bennett, 1958):

$$r^2 = \sqrt{\frac{E_k}{\rho_{Air} \ l_w}} \ \ t, \tag{2}$$

where E_k is the kinetic energy of the plasma, that is, the fraction of the total energy absorbed employed by the plasma in its expansion, ρ_{Air} is the air density, and l_w is the wire length. The above procedure allows us to express the radial expansion with an error of 0.1 mm, meanwhile the error in time determination from the streak images goes down to 50 nanoseconds.

3 Numerical method

The experiment was simulated using a simplified, 1D version of a full 3D multi-component (neutrals, ions, and electrons), two temperature, Arbitrary Lagrangian-Eulerian, Finite Volume code (Bilbao, 2006). The code includes electrical resistivity, thermal conduction, magnetic diffusion, and an equation of state (EOS) from solid to plasma obtained from different sources and models, detailed a few lines later.

The wire is coupled to the external circuit using (Rodríguez Prieto et al., 2016):

$$\frac{d\left[(L_0 + L_b)I\right]}{dt} = \frac{Q}{C} - RI - \int_b \vec{E} \bullet d\vec{l}, \tag{3}$$

where Q is the charge of the capacitor bank, C its capacity, L_0 and R are the inductance and the resistance of the concentrated elements of the circuit, respectively, L_b is the inductance calculated at the plasma boundary (b refers to the plasma boundary), $\vec{E}$ is the electric field along a path ($d\vec{l}$) on the plasma boundary (as seen in the frame fixed to the plasma), and I is the current.

The integration in time is sequential. This means that each physical process is integrated with a different uncoupled method during a time step. The solution does not depend on the integration order of the physical processes. The overall truncation error is $\mathcal{O}(\Delta x, \Delta y, \Delta z, \Delta t)$, giving a good compromise between computational efficiency and accuracy. Calculations proceed as follows:

- Hydrodynamics is integrated using the improved Predictor-Corrector method as described in [Bilbao and Bernal (2010)].
- Thermal or magnetic diffusion processes are integrated using full implicit methods.
- Mesh vertices are moved in two steps: first, a Lagragian integration, followed by a rezoning when needed.

Regarding the properties of the materials and the equation of state, we have used the following approach. A Mie-Gruneisen equation of state was used for solid and liquid, meanwhile both gas and plasma components(ions, electron and neutrals) were simulated with an ideal gas equation of state. The electrical resistivity and the thermal conductivity for solid and liquid states have been interpolated from published data (Gray, 2016), for plasma state the Spitzer conductivity was used, while for gas state a trial and error method was used, as follows. Due to the lack of data on the conductivity of metallic gas, a linear dependence with temperature was assumed, and then fitted until the simulated voltage was in a reasonable accordance with the measured experimental data. The previous model is necessary due to the fact

that the electrical behaviour of the circuit strongly depends on the electrical resistivity and the thermal conductivity of the wire.

As figure 4 shows, simulation of the current and voltage on the wire as function of time for a 50 μm Cu wire, 10 kV charging voltage, reproduces well the features obtained in the experiments. Therefore we conclude that duration of the "dark pause" depends on the low resistivity of the wire after being vaporized but not sufficiently ionized to conduct large currents. Thus, electrical properties of the gas can be adjusted until an appropriated duration of this stage is achieved.

4 Results

Typical streak images are similar in their features to the depicted in fig. 5. Plasma expansion growing with the charging voltage is clearly visible, as it is the similar duration of the light emission from the metallic plasmas in all the cases. Also, the differences on the wire evolution due to the different metals and masses of the wire are apparent in the streak pictures. Nevertheless, final plasma stage is similar in all the cases in our experiments because the surrounding medium is always atmospheric air. Synchronization of data from plasma radial expansion with electrical energy absorption of the wire-plasma system allows to observe the dynamical relation between these two processes at different charging voltages.

At low initial charging voltages and for all the metals used in this work, except for tungsten, the energy transfer from the circuit to the wire, as measured by the electrical signals, is performed in two different steps. These two steps are defined by the appearance of light emission from the plasma in the streak images. Therefore, a first stage of energy absorption takes place before the plasma formation, in a pre-plasma formation stage, with an amount of energy absorption that can be an important percentage of the total. Plasma expansion begins in the second step, were the kinetic energy of the plasma is obtained from the partial absorption of the electrical energy delivered to the wire-plasma system.

Figure 6 illustrates this process by the energy transfer and plasma expansion of a copper wire of 50 μm diameter charged at 10 kV. As the charging voltage increases, the time lapse between the two energy absorption steps is reduced, until the two steps merge into one. Therefore, with the maximum charging voltage of 25 kV the two steps are not distinguishable, as figure 7 shows for the copper wire of 100 μm diameter.

Experiments performed with tungsten wire show an unique absorption

stage even at low charging voltages. Also, due to the larger resistivity, the energy absorbed is higher than for copper, see figure 8. Nevertheless, the maximum absorbed energy, almost 20 J, is similar to the heat content at melting, 13.8 J, and far from the heat content at boiling, as table 1 indicates. Both silver and molybdenum exhibit a general behavior similar to that observed using wires of copper or tungsten, except for the time delay between the beginning of electrical energy absorption and the plasma radial expansion.

At low initial voltage all metals exhibit a delay that decreases with the increasing in the charging voltage, but at larger voltages, some unexpected tendency emerges. For molybdenum the delay becomes negative, meaning that the main energy absorption is produced after the plasma generation, defined as the moment when the self-emitted light reaches at least 5% of the maximum, as explained in section 2 of this work. Meanwhile in the case of silver wires the observed delay oscillates around zero, as fig. 9 shows.

The behavior of the delay in both metals is not easy to understand. Based on simulations previously described, we found that in all cases, the delay (when present) occurs when the wire has been melted and vaporized into a very low–ionized metallic gas state. Under this condition the resistivity is high and the current becomes very small, thus retarding the energy transfer and the posterior ionization processes. This energy transfer delay happens as long as the external resistance is smaller that the one of the metallic gas, thus is the latter the one that controls the electrical current value. Depending on the voltage, and the residual current, the Joule heating will take a shorter or longer time to heat up the gas and provide the energy necessary to start the ionization process by thermal collision of the atoms, allowing for the gas transformation into plasma. Thus, the joule heating in this early time of the electrical discharge greatly influences the current density. As a matter of fact, it is the increment of the current density the reason of the reduction in the delay between energy absorption and plasma generation whenever the charging voltages increased their values. When the charging voltage is high enough, the processes of melting, vaporizing, and ionization occurs in a short period of time, during the linear increase of the current with time, thus the radius of the plasma can be described by a self-similar approximation. Therefore, using (2), for the current density it can be written:

$$j \propto \frac{\dot{I}t}{r^2} = \sqrt{\rho_{Air}\ l_w}\ \frac{\dot{I}}{\sqrt{E_k}}, \tag{4}$$

where $\dot{I}$ is the current derivative. This means that the increase of the kinetic energy with the initial charging voltage, results in a reduction of the current

density. So the delay between the electrical energy absorption and plasma creation can grow with the initial charging voltage, in a counterintuitive way, if the ratio between current and the square root of the kinetic energy diminishes.

Simulations of the exploding wire support this interpretation. When, in the simulations, the plasma is not allowed to expand by means of artificial procedures (i.e., eliminating gas or plasma dynamics and its influence on the current density), the time between the gas and plasma formation reduces to zero.

The observed delay between the electrical energy absorption and the plasma radial expansion is correlated with the measured lower limit of the resistivity as a function of time, see figure 10. To better appreciate the differences on the time dependence of the resistivity, it has been normalized to the maximum achieved value. For a charging voltage of 10 kV, the resistivity increases until a quasi-constant plateau value, from where it decays with some peaks on the downward slope at around 1.5 μs after the beginning of the electrical discharge. When the charging voltage is settled in 15 and 20 kV, the resistivity shape changes to a single peak, which differ on the slopes between both voltages.

5 Conclusions

Variation on the synchronization between the electrical energy absorption of the plasma-wire system and the plasma formation has been observed experimentally, with values ranging from ≈ 0.0 to 2.0 μs, in the case of Copper wires. A non intuitive relation for this delay had been observed for Silver, as at 15 kV of charging voltage the delay changes its sign, interrupting the tendency to being reduced with the increase of the voltage observed with other metals. Both behaviours are understood in this work because of the interplay of the ratio between current and the square root of the kinetic energy of the plasma

Also the correlation of this delay with the shape of an lower limit to the wire resistivity has been measured. Two distinct shapes for the wire resistivity had been observed, namely a single peak with different slopes for each charging voltage, and a plateau of ≈ 0.7 μs if the charging voltage is 10 kV.

In conclusion, energy absorption in the exploding wire system for slow current rates, with values under 12 A/ns, had been experimentally observed, and the difference in behaviour with faster exploding wire systems [Grinenko

et al. (2006); Sarkisov et al. (2005a,b)] is attributed to the ratio between the current derivative passing through the wire and the root of the kinetic energy of the plasma.

Aknowlegments

This study has been partially supported by the Ministerio de Energía y Competitividad of Spain (ENE2013-45661-C2-1-P) and Junta de Comunidades de Castilla-la Mancha (EII-2014-008-P). Authors wish to thank professor Roberto Piriz for his valuable comments and suggestions.

References

I. I. Beilis, R. B. Baksht, V. I. Oreshkin, A. G. Russkikh, S. A. Chaikovskii, A. Yu Labetskii, N. A. Ratakhin, and A. V. Shishlov. Discharge phenomena associated with a preheated wire explosion in vacuum: Theory and comparison with experiment. *Physics of Plasmas*, 15(1):013501, 2008. doi: 10.1063/1.2826434.

I. I. Beilis, A. Shashurin, R. B. Baksht, and V. Oreshkin. Density and temperature distributions in the plasma expanding from an exploded wire in vacuum. *Journal of Applied Physics*, 105 (3):033301, 2009. doi: http://dx.doi.org/10.1063/1.3050343. URL `http://scitation.aip.org/content/aip/journal/jap/105/3/10.1063/1.3050343`.

F. D. Bennett. Cylindrical shock waves from exploding wires. *Physics of Fluids*, 1(4):347 – 352, 1958. doi: 10.1063/1.1705893.

F. D. Bennett, Ray Hefferlin, and Roger A. Strehlow. *Progress in high temperature physics and Chemistry. Volume II.* High-temperature exploding wires. Pergamon Press, London, 1969.

L. Bilbao and L. Bernal. Dense magnetized plasma numerical simulations. *Plasma Sources Science and Technology*, 19(3):034024, 2010. URL `http://stacks.iop.org/0963-0252/19/i=3/a=034024`.

Luis Bilbao. A threedimensional finite volume arbitrary lagrangianeulerian code for plasma simulations. *AIP Conference Proceedings*, 875 (1):467 – 472, 2006. doi: http://dx.doi.org/10.1063/1.2405990. URL `http://scitation.aip.org/content/aip/proceeding/aipcp/10.1063/1.2405990`.

K. M. Chandler, D. A. Hammer, D. B. Sinars, S. A. Pikuz, and T. A. Shelkovenko. The relationship between exploding wire expansion rates and wire material properties near the boiling temperature. *IEEE Transactions on Plasma Science*, 30(2):577 – 587, 2002. doi: 10.1109/TPS.2002.1024292.

A. W. DeSilva and J. D. Katsouros. Electrical conductivity of dense copper and aluminum plasmas. *Physical Review E*, 57(5):5945 – 5951, 1998. doi: 10.1103/PhysRevE.57.5945.

S. Efimov, A. Fedotov, S. Gleizer, V. Tz. Gurovich, G. Bazalitski, and Y. E. Krasik. Characterization of converging shock waves generated by underwater electrical wire array explosion. *Physics of Plasmas*, 15(11):112703, 2008. doi: 10.1063/1.3023156.

Theodore Gray. Photographic periodic table of the elements. http://periodictable.com
Accesed on February 2016, May 2016. URL `http://periodictable.com`.

A. Grinenko, Y. E. Krasik, S. Efimov, Fedotov G., and V. Tz. Gurovich. Nanosecond time scale, high power electrical wire explosion in water. *Physics of Plasmas*, 13(4):042701, 2006. doi: 10.1063/1.2188085.

V. Ts. Gurovich, A. Grinenko, Ya. E. Krasik, and J. Felsteiner. Simplified model of underwater electrical discharge. *Physical Review E*, 69(3):036402, 2004. doi: 10.1103/PhysRevE.69.036402.

Yakov E. Krasik, Alon Grinenko, Arkady Sayapin, Sergey Efimov, Alexander Fedotov, Viktor Z. Gurovich, and Vladimir I. Oreshkin. Underwater electrical wire explosion and its applications. *IEEE Transactions on Plasma Science*, 3(2):423 – 434, 2008. doi: 10.1109/TPS.2008.918766.

N I Kuskova, S I Tkachenko, and S V Koval. Investigation of liquid metallic wire heating dynamics. *Journal of Physics: Condensed Matter*, 9:6175 – 6184, 1997. doi: 10.1088/0953-8984/9/29/003.

M. Liverts, O. Ram, O. Sadot, N. Apazidis, and G. Ben-Dor. Mitigation of exploding-wire-generated blast-waves by aqueous foam. *Physics of Fluids*, 27(7):076103, 2015. doi: 10.1063/1.4924600.

Edward Nairne. An account of the effect of electricity in shortening wires. *Philosophical Transactions of the Royal Society of London*, 70:334 – 337, 1780.

L. B. Pankratz and Robert V. Mrazek. Thermodynamic properties of elements and oxides. *Bureau of Mines Bulletin 672*, 1983.

O. Ram and O. Sadot. Implementation of the exploding wire technique to study blast-wavestructure interaction. *Experiments in Fluids*, 53(5):1335 – 1345, 2012. doi: 10.1007/s00348-012-1339-8.

Gonzalo Rodríguez Prieto, Luis Bilbao, and Malena Milanese. Temporal distribution of the electrical energy on an exploding wire. *Laser and Particle Beams*, 34(02):263–269, 06 2016. doi: 10.1017/S0263034616000069. URL `http://journals.cambridge.org/article_S0263034616000069`.

R. Sarathi, T. K. Sindhu, S. R. Chakravarthy, Archana Sharma, and K. V. Nagsesh. Generation and characterization of nano-tungsten particles formed by wire explosion process. *Journal of Alloys and Compounds*, 475: 658 – 663, 2009. doi: 10.1016/j.jallcom.2008.07.092.

G. S. Sarkisov, K. W. Struve, and D. H. McDaniel. Effect of current rate on energy deposition into exploding metal wires in vacuum. *Physics of Plasmas*, 11(10):4573, 2004. doi: 10.1063/1.1784452.

G. S. Sarkisov, S. E. Rosenthal, K. R. Cochrane, K. W. Struve, C. Deeney, and D. H. McDaniel. Nanosecond electrical explosion of thin aluminum wire in vacuum: Experimental and computational investigations. *Physical Review E*, 71(4):046404, 2005a. doi: 10.1103/PhysRevE.71.046404.

G. S. Sarkisov, K. W. Struve, and D. H. McDaniel. Effect of deposited energy on the structure of an exploding tungsten wire core in a vacuum. *Physics of Plasmas*, 12(5):052072, 2005b. doi: 10.1063/1.1883180.

Toru Sasaki, Yuuri Yano, Mitsuo Nakajima, Tohru Kawamura, and Kazuhiko Horioka. Warm-dense-matter studies using pulse-powered wire discharges in water. *Laser and Particle Beams*, 24(3):371–380, 09 2006. doi: 10.1017/S0263034606060538.

D. Sheftman and Ya. E. Krasik. Investigation of electrical conductivity and equations of state of non-ideal plasma through underwater electrical wire explosion. *Physics of Plasmas*, 17(11):112702, 2010. doi: 10.1063/1.3497010.

J. Stephens and A. Neuber. Exploding-wire experiments and theory for metal conductivity evaluation in the sub-ev regime. *Physical Review E*, 86(6): 066409, 2012. doi: 10.1103/PhysRevE.86.066409.

Jacob C. Stephens, Andreas A. Neuber, and M. Kristiansen. Simulation of an exploding wire opening switch. IEEE, 2012. doi: 10.1109/MEGAGAUSS.2012.6781418.

Tables

Table 1: Metals, diameters, and heat content at melting and boiling points for the total mass of the wires employed in these experiments.

Metal	**Diameter (μm)**	**H_{melt} - H_{298} (J)**	**H_{boil} - H_{298} (J)**
Silver(Ag)	250	21.6	188.9
Molydbenum (Mo)	100	19.7	124.5
Copper (Cu)	50	1.4	13.0
	100	5.7	52.1
Tungsten (W)	100	13.8	94.8

Figures

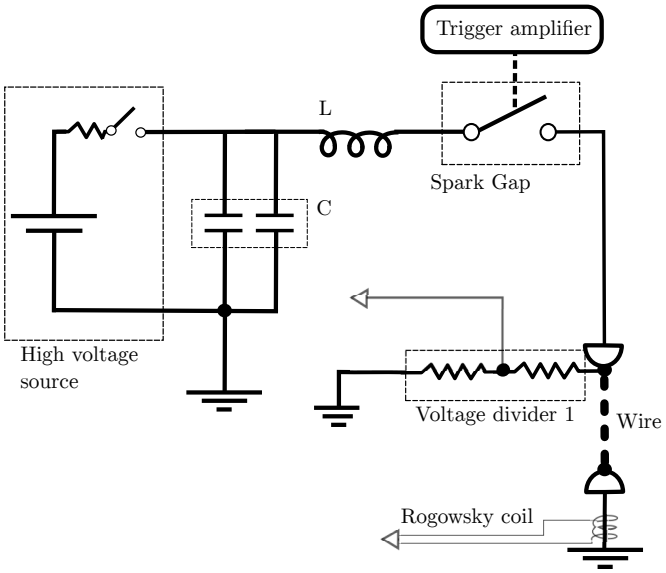

Figure 1

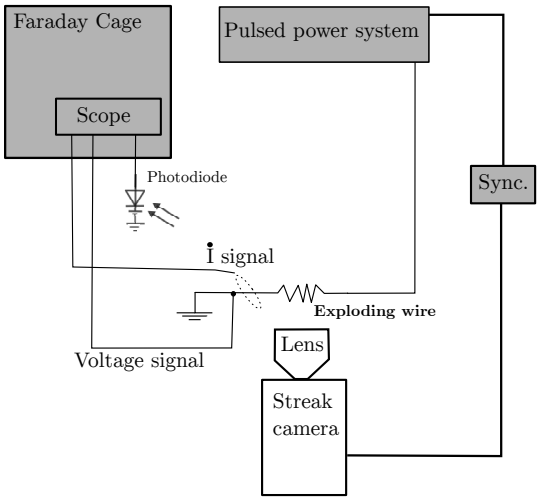
Faraday Cage
Pulsed power system
Scope
Photodiode
Sync.
I signal
Exploding wire
Lens
Voltage signal
Streak
camera

Figure 2

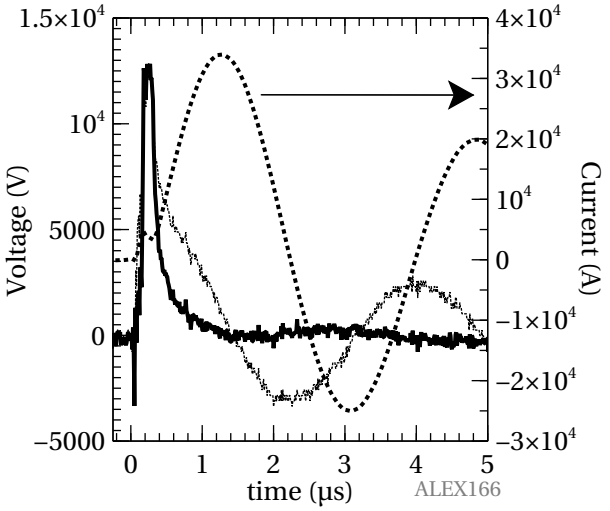
1.5×10^4
10^4
5000
0
−5000
Voltage (V)
4×10^4
3×10^4
2×10^4
10^4
0
−1×10^4
−2×10^4
−3×10^4
Current (A)
0
1
2
3
4
5
time (μs)
ALEX166

Figure 3

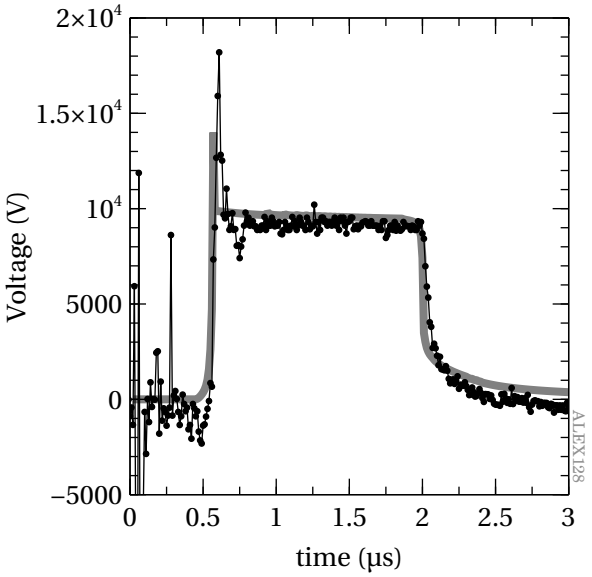
2×10^4
1.5×10^4
10^4
5000
0
−5000
Voltage (V)
0
0.5
1
1.5
2
2.5
3
time (μs)
ALEX128

Figure 4

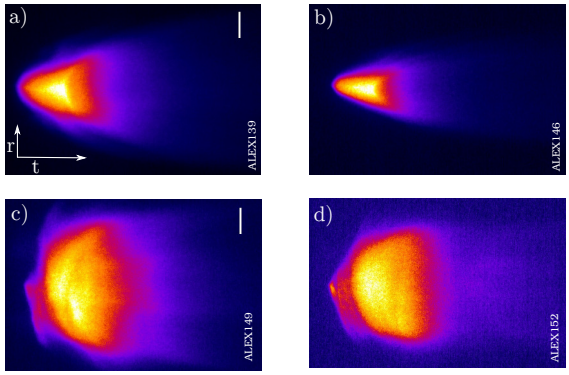

Figure 5

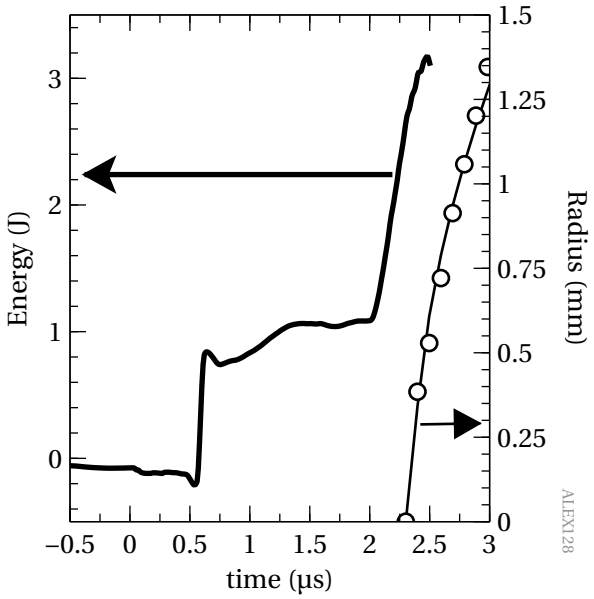
Energy (J)
Radius (mm)
time (μs)
–0.5
0
0.5
1
1.5
2
2.5
3
0
0.25
0.5
0.75
1
1.25
1.5
ALEX128

Figure 6

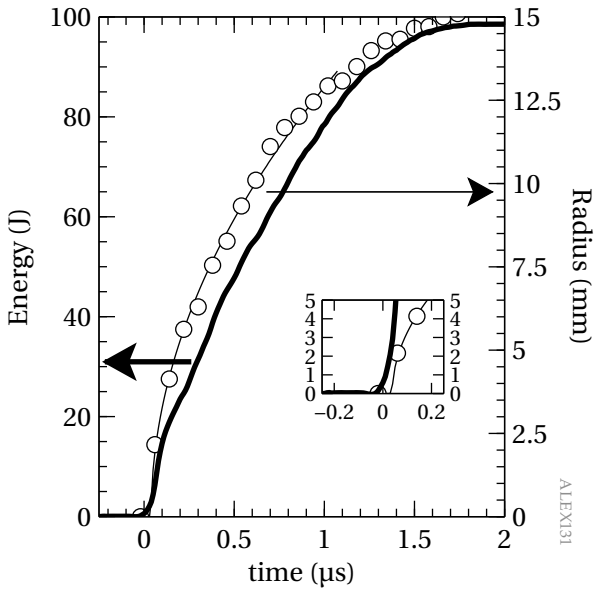

Figure 7

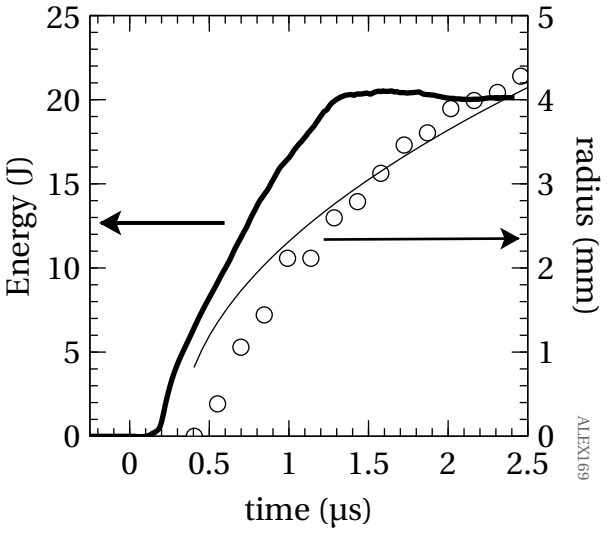
25
20
15
10
5
0
Energy (J)
5
4
3
2
1
0
radius (mm)
0
0.5
1
1.5
2
2.5
time (μs)
ALEX169

Figure 8

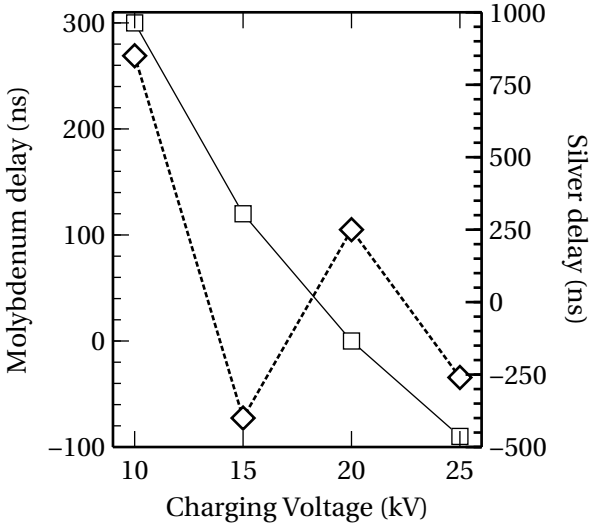
300
200
100
0
−100
1000
750
500
250
0
−250
−500
10
15
20
25
Molybdenum delay (ns)
Silver delay (ns)
Charging Voltage (kV)

Figure 9

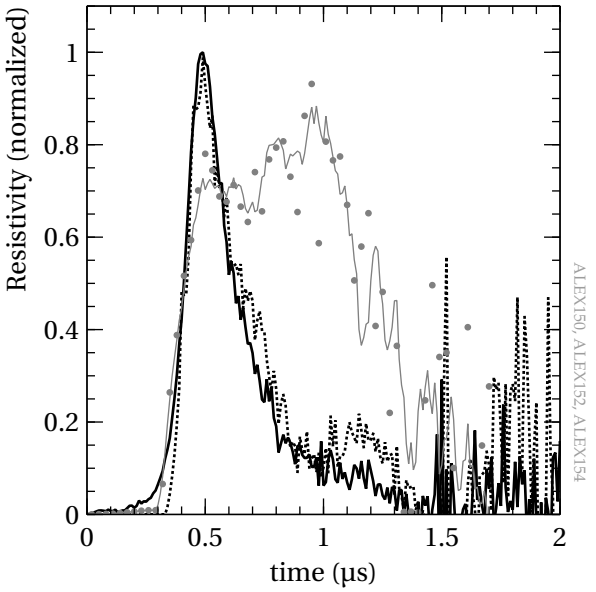
Resistivity (normalized)
1
0.8
0.6
0.4
0.2
0
0
0.5
1
1.5
2
time (μs)
ALEX150, ALEX152, ALEX154

Figure 10

Captions

Figure 1: ALEX electrical scheme. **L** and **C** mark the circuit inductance and capacitance, respectively. White arrows signal the BNC connections to the Faraday cage.

Figure 2: Scheme of the experimental setup.

Figure 3: Typical voltage, in wire(—) and the voltage divider(·····), and current(·····) signals for a tungsten wire, diameter 100 μm, with the capacitors bank charged at 15 kV.

Figure 4: Simulated (—) and experimental (–•–) voltage time evolution in a copper wire of 50 μm charged at 10 kV.

Figure 5: Molybdenum (a, b) and Silver (c, d) streak images with 25 and 10 kV charging voltage at left (a,c) and right(b, d) respectively. Bars indicate 9.6 mm and total time in horizontal dimension is 45 μs.

Figure 6: Energy(—) and radial expansion of 50 μm Copper wires(–○–) at 10 kV initial voltage charge. Hollow dots indicate experimental data and the line is the result of fitting them to the formula 2. Note the difference between the energy transfered to the wire and the heat content for the same wire, table 1. This is an indication of the incomplete wire conversion into gas or plasma, also confirmed by simulations.

Figure 7: Energy(—) and radial expansion of 100 μm Copper wires(–○–) at 25 kV initial voltage charge. The inset shows the beginning of the expansion.

Figure 8: Tungsten energy absorption and radial expansion with an initial charging voltage of 10 kV. Legend is the same that in figures 6 and 7.

Figure 9: Delay between the energy absorption and the beginning of plasma expansion at different charging voltages for Mo(—□—) and Ag(- -◇- -) wires.

Figure 10: Normalized resistivity of a silver wire of 250 μm diameter when the capacitor bank is charged with 10(–•–), 15 (—), and 20 (- - -) kV.